

## High-Resolution Resistivity Analysis of Andesite Rock Distribution in Kulon Progo's Mineral-Rich Terrain

**Rizqi Prastowo\***Department of Mining Engineering,  
Institut Teknologi Nasional Yogyakarta,  
INDONESIA**Oky Sugarbo**Department of Mining Engineering,  
Institut Teknologi Nasional Yogyakarta,  
INDONESIA**Nanda Juli Setiawan**Department of Mining Engineering,  
Institut Teknologi Nasional Yogyakarta,  
INDONESIA**Setyo Pambudi**Department of Geology Engineering,  
Institut Teknologi Nasional Yogyakarta,  
INDONESIA**Yogesh Murkute**Postgraduate Department of Geology,  
Nagpur University,  
INDIA**Vishal R. Panse**Late.B.S.ArtsProf.N.G.Science & A.G.Commerce,  
College Sakharkherda,  
INDIA**\*Correspondence: E-mail:** [rizqi@itny.ac.id](mailto:rizqi@itny.ac.id)

---

**Article Info**

---

**Article history:**

Received: March 1, 2025

Revised: June 15, 2025

Accepted: June 30, 2025

**Copyright :** © 2025 Foundae (Foundation of Advanced Education). Submitted for possible open access publication under the terms and conditions of the Creative Commons Attribution - ShareAlike 4.0 International License (CC BY SA) license (<https://creativecommons.org/licenses/by-sa/4.0/>).

---

**Abstract**

---

This study employs integrated geophysical methods to analyze the spatial distribution and subsurface geometry of andesitic rock formations in the Mujil Hill area, Kulon Progo, Yogyakarta. Electrical resistivity imaging (ERI), using a dipole-dipole configuration, was conducted to identify high-resistivity zones ( $>1000 \Omega\text{m}$ ), which are interpreted as fresh andesitic intrusions. These zones are consistently found at an average depth of 10 meters, embedded within moderately resistive volcanic breccia. Near-surface layers with low resistivity values ( $<100 \Omega\text{m}$ ) are associated with weathered volcanic deposits or unconsolidated soil. To enhance subsurface structural interpretation, resistivity data were complemented with gravity modeling, providing a more comprehensive geological assessment. The results confirm the lateral continuity and shallow emplacement of andesite bodies, highlighting their potential as a local source of construction material. This integrated geophysical approach supports sustainable mineral resource development and aligns with the objectives of the regional economic empowerment program, contributing to the responsible utilization of local geological resources.

**Keywords:** geophysical methods; electrical resistivity imaging; andesitic rock formations; gravity modeling; mineral resource development

---

**To cite this article:** Prastowo, R., Sugarbo, O., Setiawan, N. J., Pambudi, S., Murkute, Y. and Panse, V. R. (2025). High-Resolution Resistivity Analysis of Andesite Rock Distribution in Kulon Progo's Mineral-Rich Terrain. *International Journal of Hydrological and Environmental for Sustainability*, 4(2), 63-74. <https://doi.org/10.58524/ijhes.v4i2.707>

---

## INTRODUCTION

The rapid infrastructure development in Yogyakarta, including the construction of the Bedah Menoreh road and Yogyakarta International Airport (YIA), has led to a growing demand for natural construction materials. Andesite, an intermediate volcanic rock known for its durability and mechanical strength, plays a crucial role in structural applications such as road base layers, bridges, and building foundations (Czinder & Török, 2021). Kulon Progo Regency, situated in western Yogyakarta, is recognized for its substantial andesite deposits, particularly in the Mujil Hill area (Nugraha et al., 2019). Geologically, these deposits belong to the Kebobutak Formation, which formed during the Upper Oligocene. However, surface andesite exposures in this region are often highly weathered, necessitating subsurface investigation for accurate resource estimation and sustainable extraction (Listyani et al., 2023; Nishimura et al., 1986; Nugraha et al., 2019).

Traditional geological mapping methods face limitations in identifying fresh, unweathered andesite, especially when covered by layers of weathered rock or soil. As a result, geophysical methods—particularly electrical resistivity imaging (ERI) and gravity surveys—have become essential tools for subsurface characterization (Al Bulushi et al., 2016; Muthamilselvan et al., 2019; Purwanto et al., 2024). The dipole-dipole resistivity configuration is particularly useful in delineating highly resistive bodies indicative of fresh volcanic rock formations, including andesite (Hermawan & Putra, 2016; Lu et al., 2008; Nugraha et al., 2019). In volcanic terrains, resistivity values exceeding 1000  $\Omega$ m are commonly interpreted as fresh, intact andesite, distinct from weathered materials or unconsolidated deposits (Ibrahim et al., 2019; Playà et al., 2010).

This study aims to investigate the spatial distribution and subsurface configuration of andesitic rock formations in the Mujil area, Kulon Progo, using electrical resistivity data as the primary method (Martinho, 2023; Saparun et al., 2022). The necessity of this research is driven by both the increasing regional demand for local construction materials and policy directives supporting sustainable resource utilization. By identifying accessible andesite reserves, the Kulon Progo government supports the Bela Beli Kulon Progo initiative—an economic empowerment program promoting local material sourcing. Enhanced subsurface modeling can improve resource management and mitigate the environmental impacts associated with unsystematic mining activities (Cole et al., 2023; Kapugu et al., 2022).

Among available geophysical techniques, electrical resistivity imaging has demonstrated effectiveness due to its cost efficiency, non-destructive nature, and ability to provide comprehensive spatial coverage. Compared to traditional core drilling, resistivity surveys can reveal lateral and vertical lithological variations without causing extensive land disturbance (Umam et al., 2025; Yu et al., 2018). This is particularly advantageous in volcanic environments, where resistivity contrasts among different lithologies and weathering conditions enhance geological interpretation (Zheng et al., 2021).

In addition to its capability in detecting fresh and weathered rock units, the resistivity method is highly sensitive to variations in porosity, moisture content, and mineral composition. These attributes make it a valuable tool for mapping subsurface andesite distributions in complex geological settings (Al Bulushi et al., 2016; Zoysa et al., 2021). This study integrates resistivity and gravity data to produce a detailed geophysical model of the Mujil area, offering valuable insights into regional resource potential.

Ultimately, this research contributes to the sustainable development of mineral extraction, aligning infrastructure expansion with responsible geological resource management. By demonstrating the effectiveness of geophysical methods, this approach serves as a potential model for other volcanic regions balancing economic growth with environmental sustainability.

### Geological condition of research area

The Mujil Hill area in Kulon Progo, Yogyakarta, is an isolated geological feature located near Pondoworejo village in the Kalibawang sub-district. It is part of the eastern Kulon Progo mountain range, which extends in a north-south direction. The hill is primarily composed of andesite breccia, a lithology similar to the Old Andesite Formation that constitutes much of the Kulon Progo Mountains. This formation dates back to the Oligocene-Miocene period and is characterized by volcanic deposits resulting from ancient magmatic activity. The geological setting of Mujil Hill has led to speculation regarding its formation, with hypotheses suggesting either an intrusive origin or deposition from debris mass originating from the Kulon Progo Mountains (Nugraha et al., 2019).

Geophysical studies, including audio-magnetotelluric (AMT) surveys, have been conducted to investigate the subsurface characteristics of Mujil Hill. These studies aim to determine whether the hill was formed by an andesitic intrusion or by mass movement of volcanic breccia. AMT measurements along survey lines crossing the hill have revealed variations in resistivity values, which provide insights into its geological history. The results indicate that Mujil Hill was likely formed by debris mass from the Old Andesite Formation rather than by an intrusive process. This conclusion is supported by the presence of lower resistivity values beneath the hill, suggesting a composition consistent with transported volcanic material rather than a solidified magmatic intrusion (Listyani et al., 2023).

The geological complexity of Mujil Hill is further influenced by its surrounding environment. The Kulon Progo region is known for its diverse volcanic formations, including lava flows, pyroclastic deposits, and breccia layers. The presence of andesite breccia in Mujil Hill aligns with the broader volcanic history of the area, which has been shaped by multiple phases of magmatic activity and erosion. Additionally, the isolated nature of the hill raises questions about the mechanisms that led to its current topographic expression. While some researchers propose that tectonic forces played a role in its uplift, others suggest that erosional processes contributed to its distinct morphology (Nishimura et al., 1986).

Understanding the geological conditions of Mujil Hill is crucial for resource management and environmental conservation. Given its composition, the hill may hold economic potential for construction materials, particularly andesite extraction. However, sustainable mining practices must be considered to prevent excessive land degradation. Further geophysical and geological investigations could provide more detailed insights into the subsurface structure and formation history of Mujil Hill, contributing to broader studies on volcanic terrains in Indonesia.

## METHOD

The geoelectrical method, particularly electrical resistivity imaging (ERI), is one of the most widely applied geophysical techniques in subsurface exploration. It operates by injecting electrical current into the ground and measuring the resulting potential differences to determine the apparent resistivity of subsurface materials. Variations in resistivity are associated with differences in lithology, porosity, saturation, and weathering levels (Martinho, 2023; Playà et al., 2010).

A material's resistivity ( $\rho$ ) is the opposition that the material offers to the flow of electric current and is expressed in ohm-meters ( $\Omega \cdot m$ ). In inhomogeneous and isotropic media, Ohm's Law governs the relationship between voltage ( $\Delta V$ ), current ( $I$ ), and resistance ( $R$ ), and it can be mathematically expressed by equation (1) below (Prastowo et al., 2019):

$$\rho = \frac{\Delta V \cdot A}{I \cdot L} \quad \dots (1)$$

where:  $\rho$  is Resistivity ( $\Omega \cdot m$ );  $A$  is Cross-sectional area of the medium ( $m^2$ );  $L$  is distance between electrodes (m);  $\Delta V$  is potential difference (V); and  $I$  is Injected current (A). In practice, the subsurface is not homogeneous, and what is measured is the apparent resistivity ( $\rho_{a}$ ), which is influenced by the electrode array's geometry and the subsurface's complex layering. The most commonly used configuration for detailed imaging is the dipole-dipole array, which offers high lateral resolution and is effective in detecting vertical structures such as dykes or intrusive bodies (Chambers et al., 2022; Meju & Le, 2002; Prastowo et al., 2019; Sujitapan et al., 2024).

Andesite, a volcanic intrusive rock, exhibits high resistivity due to its dense, crystalline texture and low porosity. This contrasts with surrounding volcanic tuffs or weathered breccia layers with significantly lower resistivity. **Table 1** presents the typical resistivity values for andesite and other rock types.

**Table 1.** Common Resistivity Values of Subsurface Materials

Material Type	Resistivity Range ( $\Omega \cdot m$ )	Reference
Andesite (fresh)	800 – 5000	Kusmita (2021); Jayadi et al. (2019)
Volcanic Breccia	100 – 800	Khalil et al. (2020)
Weathered Tuff	10 – 100	Fattah et al. (2023)
Clay	1 – 100	Tabrizi et al. (2022)
Dry Sand	1000 – 10,000	Loke et al. (2022)
Groundwater-saturated sand	10 – 1000	Khalil et al. (2020)

These resistivity contrasts provide a reliable basis for identifying lithological boundaries and characterizing subsurface geological formations. For example, zones with resistivity exceeding 1000

$\Omega \cdot \text{m}$  in the Mujil area were interpreted as massive andesite bodies embedded within volcanic breccias based on the inversion results and geologic field validation. Recent advancements in software tools such as Res2Dinv have enhanced the ability to perform robust 2D and 3D inversions, allowing resistivity data to be interpreted with greater geological accuracy. These tools utilize iterative least-squares optimization to minimize the root-mean-square (RMS) error between observed and calculated data, resulting in reliable resistivity models (Hermawan & Putra, 2016; Nugraha et al., 2019; Siregar & Kurniawan, 2018).

### Research site

Geoelectrical surveys are also increasingly integrated with other geophysical techniques, such as gravity and magnetotellurics, to provide joint interpretations that leverage the strengths of each method. This integration in volcanic terrains like Kulon Progo is critical for distinguishing between shallow, weathered rocks and deeper intrusive bodies that may be economically significant (Meju & Le, 2002).

The geoelectrical survey was conducted using the dipole-dipole configuration to investigate subsurface resistivity variations. A total of seven survey lines were established, each with a length of 200 meters and an electrode spacing of 10 meters, to ensure comprehensive coverage and resolution of the study area (Figure 1). The measurement parameter  $n$ , which represents the depth level of investigation, ranged from 1 to 6, allowing for multi-depth resistivity profiling. Data acquisition was performed using a multichannel geoelectrical resistivity instrument, which enabled efficient and simultaneous measurements across multiple electrode pairs, thereby enhancing data quality and reducing field time (Figure 2).

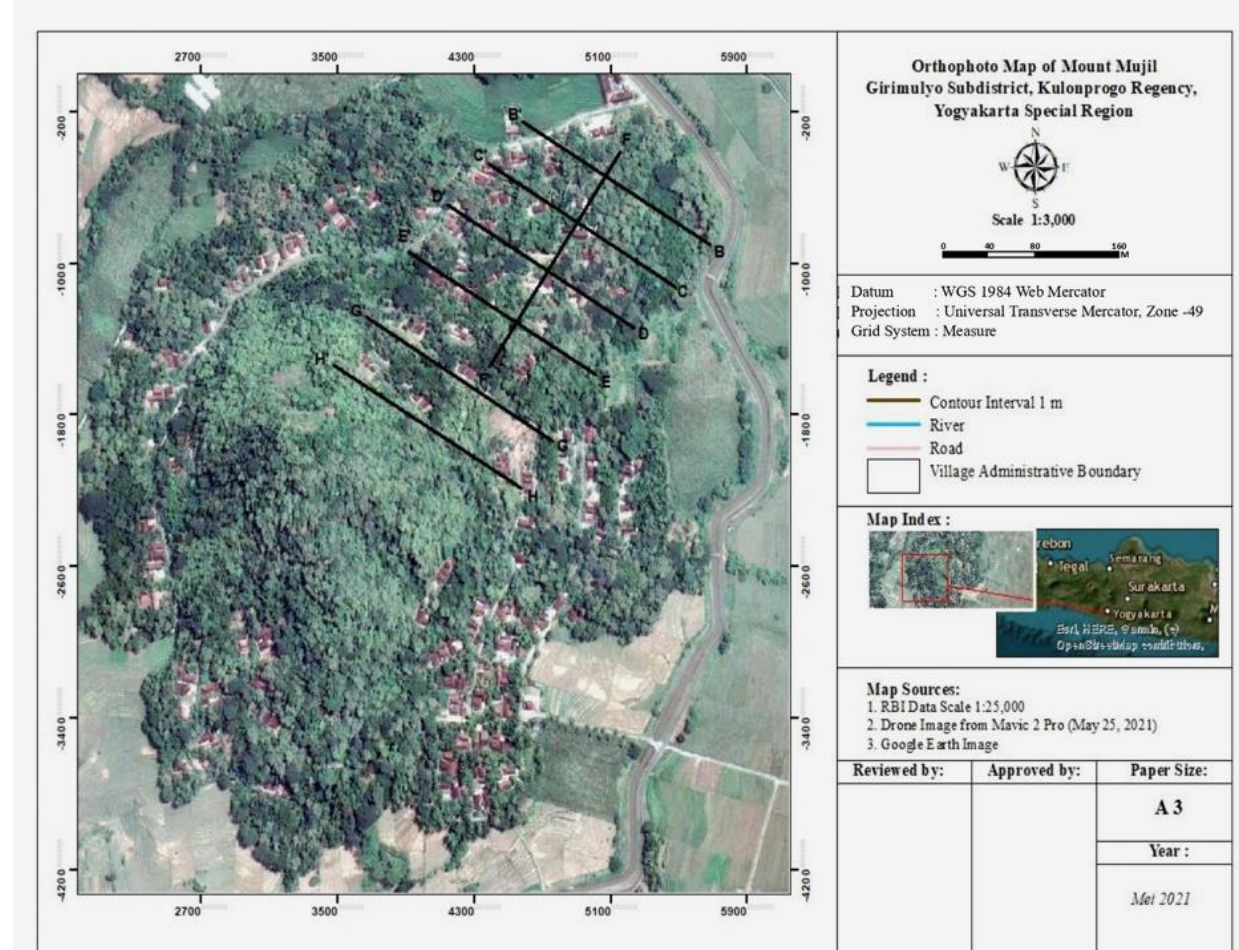


Figure 1. Geoelectrical surveys design

### Data acquisition

The data acquisition for this study involves conducting high-resolution electrical resistivity imaging (ERI) to delineate the spatial distribution of andesite rock formations in Kulon Progo's mineral-rich

terrain. The survey employs a dipole-dipole electrode configuration, which is optimal for detecting lateral and vertical resistivity variations in volcanic settings. Measurement lines are strategically positioned across suspected andesite-rich zones, with electrode spacing adjusted to ensure fine-scale resolution of subsurface geological structures. The resistivity meter records apparent resistivity values at multiple depths, allowing for detailed modeling of rock formations. Additionally, ground-truthing through geological field observations is performed to validate resistivity interpretations and correlate geophysical anomalies with actual lithological variations.

To enhance subsurface characterization, the resistivity dataset is integrated with gravity survey data, which aids in identifying density contrasts associated with different rock types. Gravity measurements are collected at regular intervals along the survey grid, providing insights into deeper geological structures beyond the reach of resistivity imaging. Data processing includes 2D inversion modeling using specialized geophysical software to generate detailed subsurface resistivity maps. The combined approach improves the accuracy of andesite rock distribution mapping, offering valuable insights into resource potential while minimizing environmental impact. This methodological framework ensures a comprehensive geophysical assessment, supporting sustainable mineral exploration and extraction strategies in Kulon Progo.



**Figure 2.** Data acquisition of geoelectrical surveys

## RESULTS AND DISCUSSION

The interpretation of geoelectrical data using the dipole-dipole configuration across eight survey lines (B through H) revealed high resistivity zones exceeding  $1000 \Omega\text{m}$  at an average depth of approximately 10 meters. These high-resistivity anomalies are consistently interpreted as andesitic rock intrusions embedded within volcanic breccia, which is characterized by intermediate resistivity values ranging from 300 to  $600 \Omega\text{m}$ . Notably, the distribution of andesite exhibits lateral continuity, especially along line G, where it extends laterally for approximately 70 meters. Zones with resistivity values below  $100 \Omega\text{m}$  are interpreted as weathered volcanic deposits, typically occurring near the surface. These findings indicate the effectiveness of the geoelectrical method in delineating subsurface andesite bodies, corroborating previous research that emphasized the high resistivity signature of unweathered andesitic rocks (Chen et al., 2020).

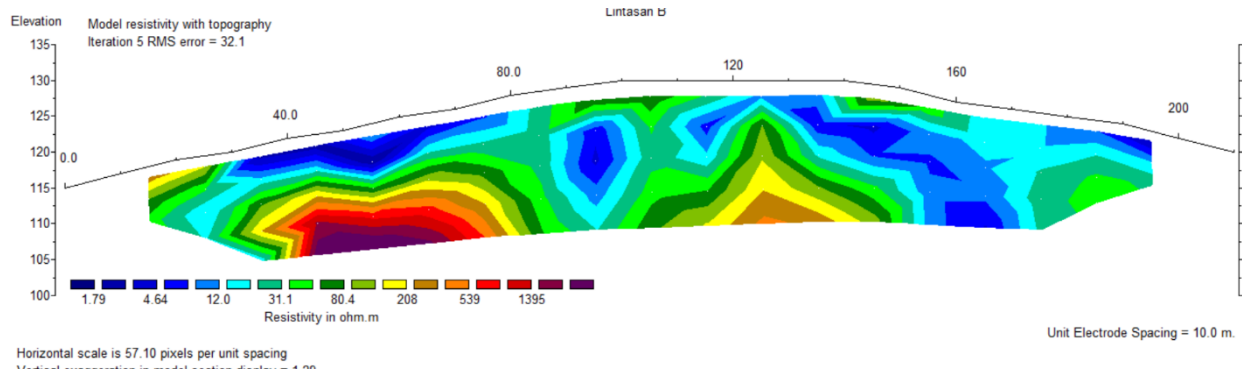


Figure 3. 2D Model Line B

**Figure 3** presents the two-dimensional resistivity model along survey line B, revealing significant subsurface variations in electrical resistivity. The model indicates a prominent high-resistivity zone exceeding  $1000 \Omega\text{m}$ , interpreted as a fresh andesitic body, represented by the purple-colored region. This zone is situated within a host of moderate-resistivity material ranging from 300 to  $536 \Omega\text{m}$ , consistent with volcanic breccia, suggesting that the andesite occurs as an intrusive body embedded within pyroclastic deposits. The andesite appears at a depth of approximately 10 meters and displays lateral continuity, indicating a sizable and coherent intrusive feature. Near-surface layers with resistivity values below  $100 \Omega\text{m}$  are interpreted as weathered volcanic material or soil cover. These resistivity patterns support the geological inference that Gunung Mujil contains a shallow andesitic intrusion, potentially suitable for exploitation as a construction material due to its intact subsurface preservation.

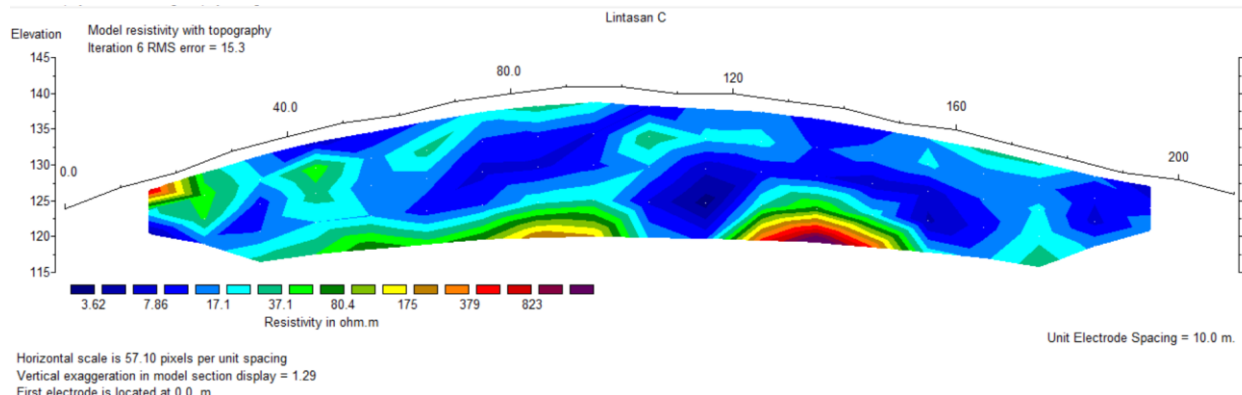


Figure 4. 2D Model line C

**Figure 4** illustrates the two-dimensional resistivity model for survey line C, showing subsurface resistivity variations consistent with the lithological characteristics observed along line B. A distinct high-resistivity zone exceeding  $823 \Omega\text{m}$ , shown in purple, is identified at approximately 10 meters and interpreted as a fresh andesitic rock. This resistive body is enveloped by materials with intermediate resistivity values ranging from 350 to  $600 \Omega\text{m}$ , indicative of volcanic breccia. The presence of andesite within breccia fragments suggests a shallow intrusive relationship, where andesite intrudes or is interbedded within pyroclastic units. Low-resistivity zones ( $<100 \Omega\text{m}$ ) near the surface are associated with weathered volcanic products or soil cover. The andesite body's lateral consistency and spatial positioning further corroborate the interpretation that Gunung Mujil hosts a continuous, shallow igneous intrusion, reinforcing its potential as a significant source of construction-grade andesite.

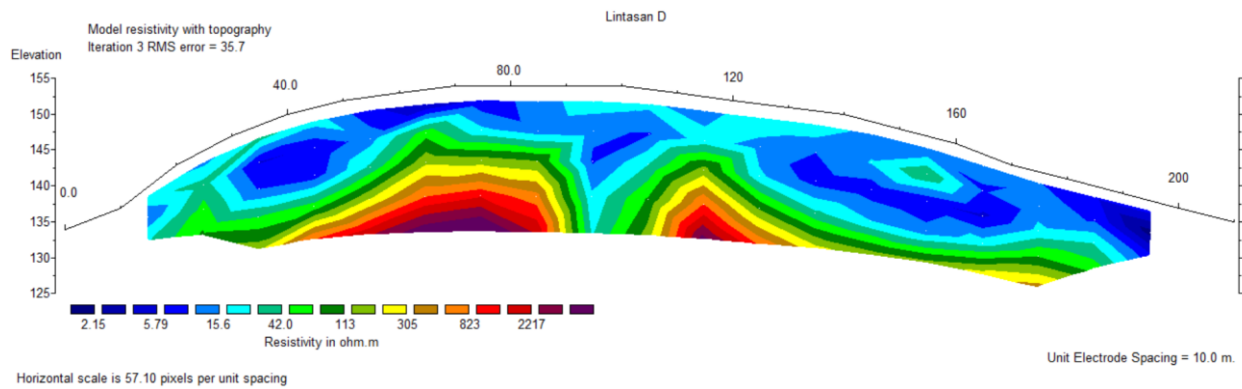


Figure 5. 2D Model line D

**Figure 5** depicts the 2D resistivity model along survey line D, highlighting a subsurface resistivity pattern that aligns with the geological expectations for andesitic intrusions in the study area. The model identifies a high-resistivity anomaly exceeding 1000  $\Omega\text{m}$ , represented in purple, as a coherent body of fresh andesite. This zone is embedded within a matrix of volcanic breccia, characterized by moderate resistivity values ranging from 305 to 600  $\Omega\text{m}$ . The andesitic unit appears at an approximate depth of 10 meters, consistent with findings from adjacent lines, and demonstrates lateral continuity suggestive of a persistent subsurface feature. The low-resistivity zones ( $<100 \Omega\text{m}$ ) near the surface likely correspond to weathered volcanic rocks or soil horizons. These geoelectrical responses reinforce the hypothesis of a shallow andesitic intrusion beneath Gunung Mujil, providing further geophysical evidence for its potential as a mineable source of volcanic rock suitable for construction materials.

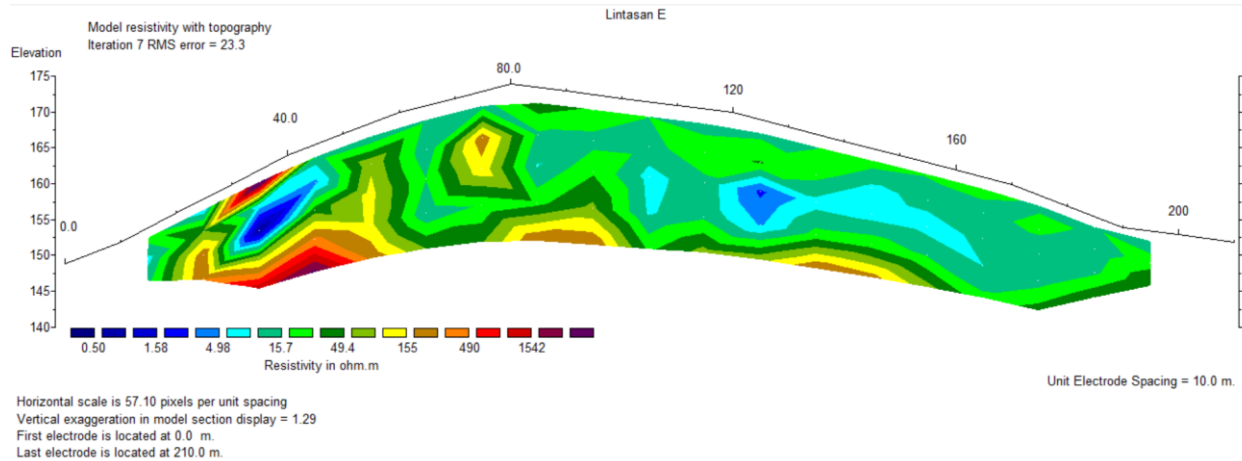
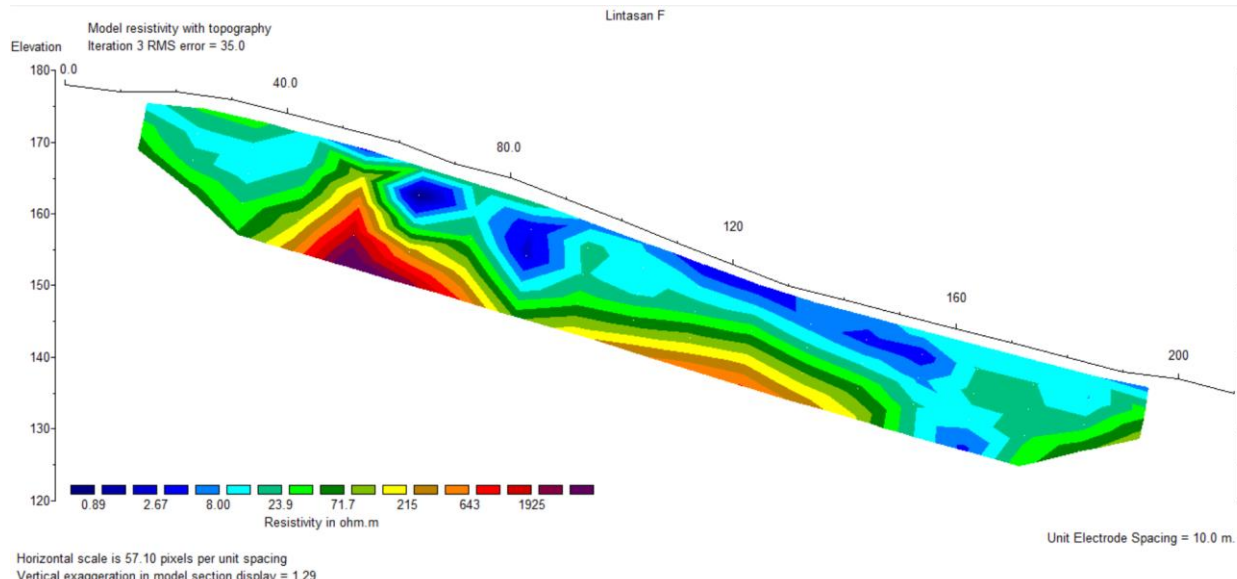
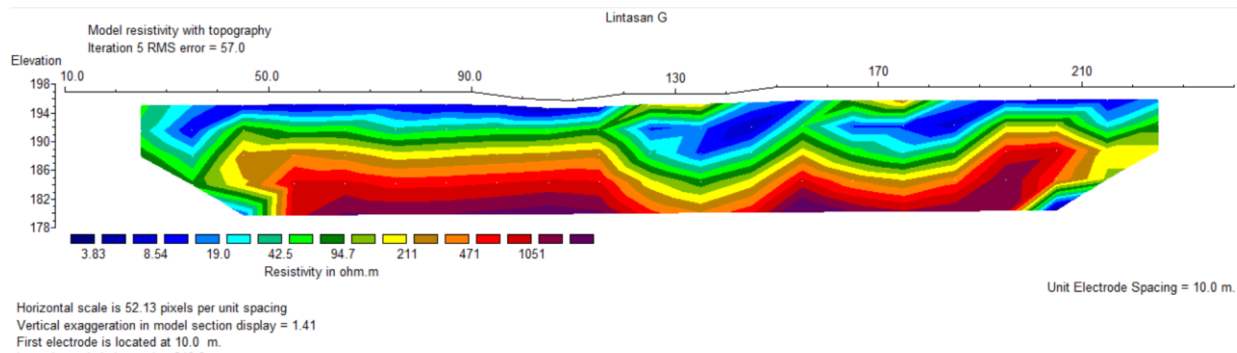


Figure 6. 2D Model Line E

**Figure 6** shows the 2D resistivity model along survey line E, revealing a subsurface profile dominated by a prominent high-resistivity zone exceeding 1000  $\Omega\text{m}$ , which is interpreted as fresh andesitic rock. This resistive body is situated within a moderately resistive host medium (350–500  $\Omega\text{m}$ ), indicative of volcanic breccia, suggesting an intrusive emplacement of andesite within pyroclastic deposits. The andesitic unit appears at a consistent depth of approximately 10 meters, supporting the continuity of this lithological feature observed across other survey lines. The near-surface layers exhibit low resistivity values ( $<100 \Omega\text{m}$ ), commonly associated with weathered volcanic material or surface soil. The uniform depth and lateral extent of the andesite anomaly along line E reinforce the interpretation of a substantial, shallow andesitic intrusion in the Gunung Mujil area, further confirming its geological and economic significance as a potential source of quarry material.

**Figure 7.** 2D Model Line F

**Figure 7** presents the 2D resistivity model for survey line F, illustrating a subsurface structure characterized by a high-resistivity zone exceeding 1000  $\Omega\text{m}$ , which is interpreted as fresh andesitic rock. This anomaly is embedded within a surrounding lithology of moderate resistivity values ranging from 215 to 600  $\Omega\text{m}$ , consistent with volcanic breccia deposits. The resistive andesite body appears approximately 10 meters, in agreement with the depth estimations from adjacent lines, and shows lateral continuity, suggesting a coherent and widespread intrusive feature. The low-resistivity zones ( $<100 \Omega\text{m}$ ) near the surface likely indicate weathered volcanic materials, soil, or clay-rich deposits. The presence of a well-defined andesitic intrusion at this depth, supported by both resistivity contrast and structural continuity, highlights the geological coherence of the intrusion and supports the area's potential for andesite resource development.

**Figure 8.** 2D Model Line G

**Figure 8** displays the 2D resistivity model along survey line G, where a substantial high-resistivity anomaly ( $>1000 \Omega\text{m}$ ) is observed, interpreted as a fresh andesitic body. This andesitic intrusion is enveloped by moderately resistive material ranging from 350 to 600  $\Omega\text{m}$ , consistent with volcanic breccia, suggesting that the andesite intrudes into or is interbedded with pyroclastic units. The resistive zone is located at an average depth of approximately 10 meters and exhibits significant lateral continuity, extending up to 70 meters along the profile. Near-surface resistivity values below 100  $\Omega\text{m}$  are attributed to weathered volcanic rocks or soil cover. The andesitic body's spatial extent and consistent depth along line G further validate the interpretation of a widespread shallow intrusion beneath Gunung Mujil, underscoring its significance as a viable andesite resource for potential quarry development.

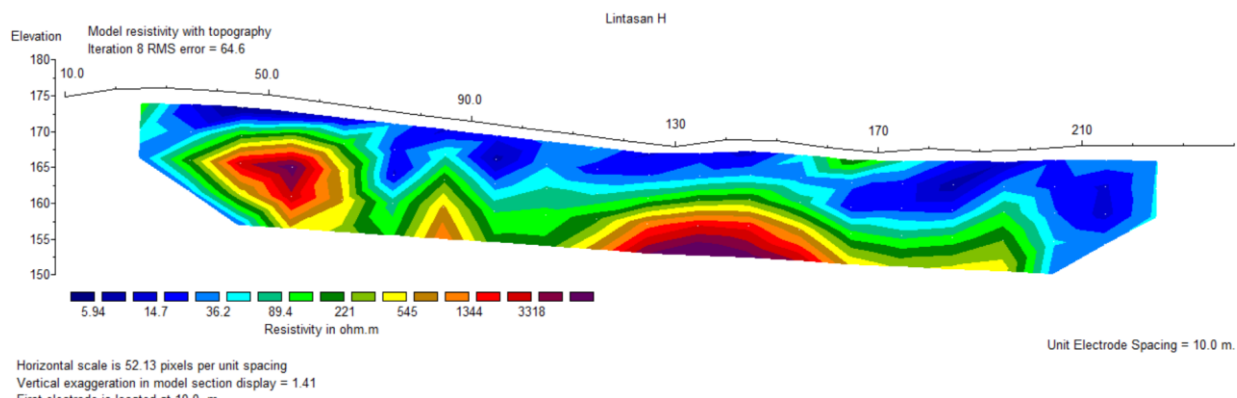


**Figure 9.** 2D Model line H

**Figure 9** presents the 2D resistivity model along survey line H, which reveals a well-defined high-resistivity anomaly exceeding 1000  $\Omega$ m, interpreted as a zone of fresh andesitic rock. This anomaly is embedded within a surrounding lithology characterized by moderate resistivity values between 350 and 600  $\Omega$ m, consistent with volcanic breccia. The andesite body appears at a depth of approximately 10 meters and demonstrates continuity along the horizontal profile, indicating a laterally extensive intrusive feature. Above this unit, low-resistivity values (<100  $\Omega$ m) dominate the near-surface, corresponding to weathered volcanic material or soil. The consistency of resistivity patterns with previous lines supports the interpretation of a shallow and coherent andesitic intrusion within the Gunung Mujil area, reinforcing its potential as a geologically viable and economically valuable source of construction-grade volcanic rock.

The interpretation of eight 2D geoelectrical resistivity profiles in the Gunung Mujil area revealed consistently high-resistivity anomalies exceeding 1000  $\Omega$ m at an average depth of approximately 10 meters. These zones are interpreted as unweathered andesitic intrusions embedded within volcanic breccia, which displayed moderate resistivity values between 300 and 600  $\Omega$ m. Near-surface zones with resistivity values below 100  $\Omega$ m were attributed to weathered volcanic deposits or soil cover. The dipole-dipole configuration proved to be particularly effective in delineating such subsurface resistive bodies, consistent with prior findings that emphasize the method's sensitivity in distinguishing lithological variations in volcanic terrains (Anuar et al., 2021).

The lateral continuity and consistent depth of the high-resistivity zones across all surveyed lines indicate the presence of a coherent and extensive subsurface andesitic unit. These geophysical signatures align well with geological field observations, reinforcing the reliability of an integrated interpretation framework that combines resistivity, gravity, and surface geological data. This integrative approach enhances subsurface resolution and reduces interpretation ambiguity, which is crucial for sustainable mineral resource planning (Thoreau & Prayer, 2000).

Furthermore, the combined use of resistivity and gravity data provided a refined subsurface model that clearly distinguished between weathered and fresh rock zones, facilitating a more accurate spatial estimation of andesite distribution. This methodology supports the sustainable development of construction-grade volcanic rock by enabling targeted resource extraction with minimal environmental impact. The findings are consistent with other recent studies in volcanic settings that advocate for multi-method geophysical approaches to reduce subsurface uncertainty and guide responsible mineral exploitation (Jamal & Singh, 2018; Karingithi, 2009; Schack & Foundation, 2015).

## CONCLUSION

The interpretation of geoelectrical resistivity data using the dipole-dipole configuration has successfully delineated high-resistivity zones (>1000  $\Omega$ m) at an average depth of 10 meters, which are consistently identified as fresh andesitic intrusions. These anomalies demonstrate significant lateral continuity, particularly along survey line G, where the intrusive body extends laterally for approximately 70 meters. The presence of moderately resistive volcanic breccia (300–600  $\Omega$ m) surrounding these intrusions further supports their emplacement within pyroclastic deposits. Additionally, near-surface low-resistivity zones (<100  $\Omega$ m) were interpreted as weathered volcanic

materials or soil cover, reinforcing the stratigraphic consistency observed across survey lines. The findings validate the effectiveness of geoelectrical resistivity methods in subsurface geological mapping, particularly in identifying andesitic rock formations embedded within brecciated volcanic layers. The lateral continuity and consistent depth of these resistive anomalies indicate a coherent and widespread subsurface andesitic unit beneath Gunung Mujil. This conclusion aligns with prior geological studies that emphasize the unique resistivity signature of unweathered andesitic rocks, demonstrating the reliability of electrical resistivity imaging for lithological characterization in volcanic settings. Furthermore, the integration of resistivity and gravity data has enhanced subsurface resolution and reduced interpretation uncertainties. This multi-method geophysical approach enables more precise spatial estimations of resource distribution, ensuring that mineral exploration and extraction can be conducted sustainably. By distinguishing between fresh and weathered rock zones, the study provides valuable insights into andesite resource potential, contributing to efficient material utilization while minimizing environmental impact. The research outcomes underscore the importance of geophysical methods in supporting responsible mineral exploitation and sustainable development. The well-defined andesitic intrusions identified in Gunung Mujil highlight its economic potential as a source of high-quality construction material. Future studies integrating additional geophysical techniques, such as seismic surveys or magnetotelluric analysis, could further refine subsurface interpretations and expand geological understanding for broader applications in volcanic regions.

### ACKNOWLEDGMENT

The authors would like to express their sincere gratitude to Institut Teknologi Nasional Yogyakarta (ITNY) for the financial support provided for this research. The institution's funding and continuous encouragement greatly contributed to the successful completion of this work.

### CONFLICTS OF INTEREST

The authors declare no conflict of interest concerning the publication of this article. The authors also confirm that the data and the article are free of plagiarism.

### REFERENCES

Al Bulushi, A. M., Al Wardi, M., Al Shaqsi, B., & Sundararajan, N. (2016). Mapping of subsurface fault structures by VLF-EM method in Al Khoud area, Muscat, Sultanate of Oman. *Arabian Journal of Geosciences*, 9(5). <https://doi.org/10.1007/s12517-016-2331-z>

Anuar, M. N. A., Arifin, M. H., Baioumy, H., & Nawawi, M. (2021). A geochemical comparison between volcanic and non-volcanic hot springs from East Malaysia: Implications for their origin and geothermometry. *Journal of Asian Earth Sciences*, 217(August 2020), 104843. <https://doi.org/10.1016/j.jseaes.2021.104843>

Chambers, J., Holmes, J., Whiteley, J., Boyd, J., Meldrum, P., Wilkinson, P., Kuras, O., Swift, R., Harrison, H., Glendinning, S., Stirling, R., Huntley, D., Slater, N., & Donohue, S. (2022). Long-term geoelectrical monitoring of landslides in natural and engineered slopes. *Leading Edge*, 41(11), 768–767. <https://doi.org/10.1190/tle41110768.1>

Chen, X., Zheng, Y., Gao, S., Wu, S., Jiang, X., Jiang, J., Cai, P., & Lin, C. (2020). Ages and petrogenesis of the late Triassic andesitic rocks at the Luerma porphyry Cu deposit, western Gangdese, and implications for regional metallogeny. *Gondwana Research*, 85, 103–123. <https://doi.org/10.1016/j.gr.2020.04.006>

Cole, M. J., Mthenjane, M., & van Zyl, A. T. (2023). Assessing coal mine closures and mining community profiles for the 'just transition' in South Africa. *Journal of the Southern African Institute of Mining and Metallurgy*, 123(6), 329–342. <https://doi.org/10.17159/2411-9717/2689/2023>

Czinder, B., & Török, Á. (2021). Strength and abrasive properties of andesite: relationships between strength parameters measured on cylindrical test specimens and micro-Deval values—a tool for durability assessment. *Bulletin of Engineering Geology and the Environment*, 80(12), 8871–8889. <https://doi.org/10.1007/s10064-020-01983-9>

Fattah, N. M., Khalil, M. A., & Aboelkhair, H. (2023). Integration of geoelectrical and geotechnical data for evaluating subsurface lithology. *Environmental Earth Sciences*, 82, 357. <https://doi.org/10.1007/s12665-023-10918-w>

Hermawan, O. R., & Putra, D. P. E. (2016). The Effectiveness of Wenner-Schlumberger and Dipole-dipole Array of 2D Geoelectrical Survey to Detect The Occurring of Groundwater in the Gunung Kidul Karst Aquifer System, Yogyakarta, Indonesia. *Journal of Applied Geology*, 1(2), 71–81.

Ibrahim, E., Gultaf, H., Saputra, H., Agustina, L. K., Rahmada, V., Suhendi, C., Sudibyo, M. R. P., & Rizki, R. (2019). Preliminary Result: Identification of Landslides Using Electrical Resistivity Tomography Case Study Mt. Betung. *Journal of Science and Application Technology*, 2(1), 107–110. <https://doi.org/10.35472/281455>

Jamal, N., & Singh, N. P. (2018). Identification of fracture zones for groundwater exploration using very low frequency electromagnetic (VLF-EM) and electrical resistivity (ER) methods in hard rock area of Sangod Block, Kota District, Rajasthan, India. *Groundwater for Sustainable Development*, 7(May), 195–203. <https://doi.org/10.1016/j.gsd.2018.05.003>

Jayadi, H., Meidji, I. U., & Tang, B. Y. (2019). Identifying Andesite Rock Sources Using Geoelectrical Resistivity in Loli, Donggala Regency, Central Sulawesi. *Journal of Physical Science and Engineering*, 4(2), 45–54.

Kapugu, E. R., Adnyano, A. A. I. A., Prastowo, R., Zamroni, A., Kaur, M., & Brahme, N. (2022). The Effectiveness of Sump Dimension Design: A Case Study in Nickel Mining. *International Journal of Hydrological and Environmental for Sustainability*, 1(1), 41–53. <https://doi.org/10.58524/ijhes.v1i1.69>

Karingithi, C. W. (2009). Chemical geothermometers for geothermal exploration.

Khalil, M. A., El-Qady, G., & Aboelkhair, H. (2020). Electrical resistivity imaging for mapping groundwater contamination and geological structures. *Journal of Applied Geophysics*, 182, 104155.

Kusmita, T. (2021). 2D Electrical Resistivity Imaging to Determine Depth of Andesite Spreading at Tanjung Batu, Jambi. *IOP Conference Series: Earth and Environmental Science*, 12046.

Listyani, R. A. T.-, Prabowo, I. A., & De Jesus, A. A. (2023). Aquifer Potential Analysis Based On Hydrostratigraphy and Geological Lineament In Kokap Region, Kulon Progo, Yogyakarta, Indonesia. *International Journal of Hydrological and Environmental for Sustainability*, 2(2), 50–64. <https://doi.org/10.58524/ijhes.v2i2.197>

Loke, M. H., Wilkinson, P. B., & Chambers, J. E. (2022). Recent developments in electrical imaging and advances in 3D inversion techniques. *Surveys in Geophysics*, 43, 55–80. <https://doi.org/10.1007/s10712-021-09645-9>

Lu, Z., Dai, J., Song, X., Wang, G., & Yang, W. (2008). Facile synthesis of Fe3O4/SiO2 composite nanoparticles from primary silica particles. *Colloids and Surfaces A: Physicochemical and Engineering Aspects*, 317(1–3), 450–456. <https://doi.org/10.1016/j.colsurfa.2007.11.020>

Martinho, E. (2023). Electrical Resistivity and Induced Polarization Methods for Environmental Investigations: an Overview. In *Water, Air, and Soil Pollution* (Vol. 234, Issue 4). Springer International Publishing. <https://doi.org/10.1007/s11270-023-06214-x>

Meju, M. A., & Le, L. (2002). Geoelectromagneticexploration For Natural Resources:Models, Case Studies and Challenges. *Surveys in Geophysics*, 23, 133–205.

Muthamilselvan, A., Rajasekaran, N., & Suresh, R. (2019). Mapping of hard rock aquifer system and artificial recharge zonation through remote sensing and GIS approach in parts of Perambalur District of Tamil Nadu, India. *Journal of Groundwater Science and Engineering*, 7(3), 264–281. <https://doi.org/10.19637/j.cnki.2305-7068.2019.03.007>

Nishimura, S., Nishida, J., Yokoyama, T., & Hehuwat, F. (1986). Neo-tectonics of the Strait of Sunda, Indonesia. *Journal of Southeast Asian Earth Sciences*, 1(2), 81–91. [https://doi.org/10.1016/0743-9547\(86\)90023-1](https://doi.org/10.1016/0743-9547(86)90023-1)

Nugraha, A. S., Darsono, D., & Legowo, B. (2019). Identification of the distribution of andesite rocks in Kalirejo Village, Kokap District, Kulon Progo Regency, Special Region of Yogyakarta based on geoelectrical tomography data. *Journal of Physics: Conference Series*, 1153(1). <https://doi.org/10.1088/1742-6596/1153/1/012019>

Playà, E., Rivero, L., & Himi, M. (2010). Electrical resistivity tomography and induced polarization techniques applied to the identification of gypsum rocks ‡. *Near Surface Geophysics*, 249–257. <https://doi.org/10.3997/1873-0604.2010009>

Prastowo, R., Huda, S., Umam, R., Jermitsittiparsert, K., Prasetyo, A. E., Tortop, H. S., & Syazali, M. (2019). Academic Achievement and Conceptual Understanding of Electrodynamics: Applications Geoelectric Using Cooperative Learning Model. *Jurnal Ilmiah Pendidikan Fisika Al-Biruni*, 8(2), 165–175. <https://doi.org/10.24042/jipf.albiruni.v0i0.4614>

Purwanto, M. S., Susilo, A., Bahri, A. S., Naba, A., Sari, U. I., & Almais, A. T. W. (2024). Mapping Underground River Flows in karst Areas with the VLF-EM Method (Case Study of the Krawak Region, Singgahan Tuban). *IOP Conference Series: Earth and Environmental Science*, 1307(1). <https://doi.org/10.1088/1755-1315/1307/1/012005>

Saparun, M., Akbar, R., Marbun, M., Dixit, A., & Saxena, A. (2022). Application of Induced Polarization and Resistivity to the Determination of the Location of Minerals in Extrusive Rock Area, Southern Mountains of Java, Indonesia. *International Journal of Hydrological and Environmental for Sustainability*, 1(3), 108–119. <https://doi.org/10.58524/ijhes.v1i3.137>

Schack, S., & Foundation, K. (2015). The Effectiveness of E-Learning : An Explorative and Integrative Review of the Definitions , Methodologies and Factors that Promote e-Learning Effectiveness ResearchLAB : IT and Learning Design , Dep . of Learning and Philosophy , Aalborg. *The Electronic Journal of E-Learning*, 13(4), 278–290.

Siregar, R. N., & Kurniawan, W. B. (2018). 2D Interpretation Of Subsurface Hot Spring Geothermal Structure In Nyelanding Village Through Schlumberger Geoelectricity. *Jurnal Ilmiah Pendidikan Fisika Al-BiRuNi*, 07(April), 81–87. <https://doi.org/10.24042/jipf.albiruni.v7i1.2324>

Sujitapan, C., Kendall, J. M., Chambers, J. E., & Yordkayhun, S. (2024). Landslide assessment through integrated geoelectrical and seismic methods: A case study in Thungsong site, southern Thailand. *Heliyon*, 10(2). <https://doi.org/10.1016/j.heliyon.2024.e24660>

Tabrizi, M., Yazdani, M. R., & Moayedi, H. (2022). Application of geoelectrical techniques in engineering site investigation and groundwater studies. *Bulletin of Engineering Geology and the Environment*, 81, 276. <https://doi.org/10.1007/s10064-021-02518-1>

Thoreau, H. D., & Prayer, Y. I. (2000). *Rocks & Minerals* (p. 38).

Umam, R., Junaidi, R., Syazali, M., Farid, F., Saregar, A., & Andiyan, A. (2025). Optimization of Piper Trilinier Diagram Using Lithium Isotope Systematics : An Application for Detecting the Contribution of Geothermal Water from Aso Caldera after Earthquake 2016 in Kumamoto Aquifer , Japan. *Indonesian Journal of Science & Technology*, 10(1), 159–170.

Yu, L., Rozemeijer, J., Van Breukelen, B. M., Ouboter, M., Van Der Vlugt, C., & Broers, H. P. (2018). Groundwater impacts on surface water quality and nutrient loads in lowland polder catchments: Monitoring the greater Amsterdam area. *Hydrology and Earth System Sciences*, 22(1), 487–508. <https://doi.org/10.5194/hess-22-487-2018>

Zheng, H., Luo, J., Zhang, Y., Feng, J., Zeng, Y., & Wang, M. (2021). Geological Characteristics and Distribution of Granite Geothermal Reservoir in Southeast Coastal Areas in China. *Frontiers in Earth Science*, 9(August), 1–18. <https://doi.org/10.3389/feart.2021.683696>

Zoysa, R. S. De, Schöne, T., Herbeck, J., Illigner, J., Haghghi, M., Simarmata, H., Porio, E., Rovere, A., & Hornidge, A. K. (2021). The “wickedness” of governing land subsidence: Policy perspectives from urban southeast Asia. *PLoS ONE*, 16(6 June), 1–25. <https://doi.org/10.1371/journal.pone.0250208>